厚生労働科学研究委託費（難治性疾患実用化研究事業）
委託業務成果報告（業務項目）

疾患特異的 iPS 細胞由来分化細胞を用いた遺伝子発現解析

担当責任者　矢野 真人 慶應義塾大学医学部生理学教室 講師

研究要旨　患者由来 iPS 細胞から誘導した神経系前駆細胞/幹細胞を含むニューロスフェアを用いた高解像度トランスクリプトーム解析の開発を目指し、今回、FUS 遺伝子に変異を有する家族性の筋萎縮症側索硬化症(ALS)の患者２名から作製した iPS から誘導した運動ニューロン前駆細胞を豊富に含むニューロスフェアを用いたエクソンアレイ解析を行い、病態関連遺伝子群を同定した。

A. 研究目的

成人発症の遺伝性神経疾患の原因は、ごく僅かな遺伝子発現異常の蓄積に伴う可能性が示唆されている。これら難病の病態解明には、iPS 細胞技術を始めとする病態解析系の開発と同様に遺伝子発現異常の高解像度解析技術の開発もまた挑戦的かつ急務となっている。そこで本研究では、iPS 細胞由来分化細胞を用いたトランスクリプトーム解析技術の開発を行う事を目的とした。

B. 研究方法

家族性 ALS の原因遺伝子 FUS に変異を持つ2名の患者線維芽細胞より iPS 細胞を樹立した。次に、3 種類の健常者由来 iPS 細胞をコントロールとして、家族性 ALS 特異的 iPS 細胞から運動ニューロン前駆細胞を豊富に含むニューロスフェアへの分化誘導を行った。運動ニューロンへの分化能、分化効率を検証後、ニューロスフェアから精製した全 RNA を用いて、Affymetrix 社の Exon アレイ解析を行った。RNA 制御因子である FUS が直接制御しいている遺伝子による病態の原因を追跡するため、Gene Yeo らのグループで発表されている CLIP-seq データの再解析を行い、我々の発現解析と統合解析を行った。また、遺伝子発現変動に伴う病態関連性を示す表現型解析も合わせて行った。

（倫理面への配慮）

ヒト細胞からのヒト iPS 細胞の樹立と樹立した iPS 細胞を用いた研究に関しては、慶應義塾大学医学部生命倫理委員会において、「神経疾患患者からの iPS 細胞の樹立とそれを用いた疾患解析に関する研究」として承認されており、それに基づいて研究計画を立案・遂行している。

C. 研究結果

Exon アレイ解析の結果、健常者と患者由来のニューロスフェア間で転写産物レベルにおいて発現に有意に変動を示す 159 遺伝子を同定した。159 遺伝子のうち 78%が患者由来ニューロスフェアで発現上昇を示す結果となった。また、CLIP-seq データの low data の再解析を行った。それぞれのユニークリード Tag 同士が 3 塩基以上の重複が認められ、かつ 20tags 以上を有し Peak Hight10 以上もつクラスター領域を一つの FUS-RNA 結合領域と定義した。この結果から、FUS が直接 RNA に結合する領域の 72.6%がイントロン配列であること、また 13.6%が 3’ 非翻訳領域であることが分かった。FUS 結合クラスターを有する 1,558 遺伝子を FUS の直接標的遺伝子として、患者由来のサンプルで発現上昇を示す Exon アレイデータの遺伝子群と統合解析すると 90%以上が発現上昇を示す結果となった。また、FUS が直接制御している遺伝子群の中には、患者由来サンプルにおいて RNA プロセシング異常を示すいくつかの選択的エクソンも同定された。これら変動する遺伝子群について、RNA プロセシング異常については semi-quantitative RT-PCR 法及び RNA 発現変動については qRT-PCR 法を用いて確証実験を行

いデータの有効性が得られた。

さらに、患者由来 iPS より分化させた運動ニューロンを用いた細胞生物学的解析を進めている。特に FUS 蛋白質の局在性の解析で、ある条件下において、いくつかの病態関連性の高い表現型が得られている。

D. 考察

これまで他のグループによる FUS の機能解析で、FUS が基本的転写因子や RNA ポリメラーゼ II との相互作用すること、またプロモーター領域の逆向きのアンチセンス RNA と相互作用すること、いずれの研究結果においても、FUS が転写抑制性に働いているとの報告がある。今回、C 末端領域にアミノ酸変異を有する患者由来 iPS から分化誘導した細胞において、有意に変動を示す遺伝子の転写レベルが上昇していることを考えると、変異型 FUS の発現により標的遺伝子群に対する FUS の機能の一部異常が反映している可能性が考えられる。実際、我々の分化誘導系を用いた細胞生物学的解析においても患者由来の細胞において FUS 蛋白質の細胞内局在に一部の異常が見られるなどの表現型が得られている。一つの可能性として、この表現型は通常の分化した運動ニューロンでは軽微な差であることから、何らかのストレス等の刺激に対する感受性の差を示すものであると考察される。つまり、今回得られたデータセットは、ごく幼弱期の運動ニューロン（前駆体）での発現変化を捉えていると同時に、患者由来細胞の脆弱性を示す遺伝子群、また、神経疾患を引き起こす早期の診断マーカーとしての有効性も示唆される。つまり、患者由来 iPS 細胞から誘導した分化系を用いた解析が、よりよい疾患ヒストリーを *in vitro* で追跡できる病態モデルとして可能性を示すものであり、また今回、その遺伝子発現レベルでの解析として有用な系が構築されつつある段階にあるといえる。

E. 結論

患者由来 iPS 細胞から誘導した細胞を用いた Exon アレイを用いた遺伝子発現解析を行って来た。これまで家族性 ALS 由来細胞の解析において原因遺伝子の機能に反映した遺伝子発現異常を検出することに成功している。

F. 健康危険情報

特になし

G. 研究発表

１．論文発表

1. **Hayashi S, Yano M, Igarashi M, Okano HJ, Okano H,** Alternative role of HuD splicing variants in neuronal differentiation, *Journal of Neuroscience Research* 93(3):399-409 2015
2. **Yano M*, Ohtsuka T, Okano H*:** RNA-binding protein research with transcriptome-wide technologies in neural development *Cell and Tissue Research* 359(1):135-144 2015 (*Corresponding author)
3. **矢野真人、岡野栄之** カンデル神経科学 PRINCIPLES OF NEURAL SCIENCE Fifth Edition Chapter3「遺伝子と行動」翻訳担当 2014年 5月
4. **大塚貴文、矢野真人、 岡野栄之**: 脳内における蛋白質-RNA相互作用の検出とその応用 Medical Science Digest 6月臨時増刊号 RNA疾患 2014年5月

２．学会発表

1. **矢野真人、古家育子、大塚貴文、坂野聡重、矢野佳芳、ダーネル・ロバート、岡野栄之** Transcriptome-wide mapping of Msi1-RNA interaction uncovers multi-layered RNA regulation by Msi1 in brain 第 16 回日本 RNA 学会 名古屋 2014 年 7 月
2. **岡野栄之、矢野真人**、Musashi, a post-transcriptional regulator of stem cells functions 第 37 回日本神経科学学会 横浜 2014 年 9 月
3. **矢野真人、ダーネル・ロバート、岡野栄之**、Transcriptome wide mapping of Msi1-RNA interaction in neural stem cell 第 37 回日本分子生物学会 横浜 2014 年 12 月
4. **Yano M, Koya I, Ohtsuka T, Banno S, Yano Y, Darnell RB, Okano H** HITS-CLIP reveals multi-layered RNA regulation by translational

regulator Msi1 in brain Cold Spring Harbor Meeting 2014 年 9 月 New York, USA

5. **一柳直希、藤崎央子、矢野真人、岡田洋平, 割田仁、青木正志、赤松和土、岡野栄之** 疾患由来 iPS 細胞を用いた家族性筋萎縮性側索硬化症の病態解析 第 14 回日本再生医療学会 横浜 2015 年 3 月
6. **大塚貴文、矢野真人、坂野聡重、芝田晋介、岡野栄之** Roles of neuronal RNA binding protein Elavl2 in the brain 第57回日本神経化学会 奈良 2014 年 9 月

H. 知的財産の出願・登録状況

１．特許取得・出願

なし

２．実用新案登録

なし

３．その他

なし

厚生労働科学研究委託費（難治性疾患実用化研究事業）
委託業務成果報告（業務項目）

SBMA と筋萎縮性側索硬化症におけるヒトの病理組織学的変化の比較検討

担当責任者　吉田眞理　愛知医科大学加齢医科学研究所　教授

研究要旨　SBMA と ALS の患者剖検病理標本を用いた組織病理学的検討を行い、下位運動ニューロンと骨格筋の病理変化を比較検討した。SBMA と ALS では下位運動ニューロンの中枢での細胞体と軸索脱落、末梢効果器の骨格筋の変性には質的な相違がある。SBMA では神経再支配が有効におこり、骨格筋は代償性肥大を示すが、ALS では骨格筋の神経原性筋萎縮は前角細胞の脱落にほぼ並行する萎縮を示す。治療戦略として運動ニューロンの救済に加えて、効果器である骨格筋の保護や刺激なども病態を変えうる可能性があり、iPS 細胞での検証が必要である。

A. 研究目的

iPS を用いた疾患モデルの構築と病態解析には、ヒトの病理像との対比が重要となってくる。球脊髄性筋萎縮症（SBMA）は、CAG リピートの異常伸長による細胞傷害をきたす遺伝性トリプレットリピート病であり、孤発性 ALS は核内蛋白である TAR DNA binding protein 43 kDa（TDP-43）の異常リン酸化と凝集により、細胞内に TDP-43 凝集体が蓄積され、ともに運動ニューロンが脱落変性する病態を示す。病理組織学的に SBMA と ALS の類似点、相違点を明確にする。

B. 研究方法

対象は SBMA 死亡時 62 歳、66 歳、74 歳男性、経過はそれぞれ 27 年、21 年、24 年、ALS 死亡時年齢 65 歳女性、73 歳男性、68 歳男性、経過 1 年 6 ヶ月、7 ヶ月、1 年 3 ヶ月。下位運動ニューロンの細胞脱落とグリアの反応、骨格筋の萎縮を対比検討した。

（倫理面への配慮）剖検例はすべて遺族の同意が文書で得られている。

C. 研究結果

SBMA、ALS とも症例毎の差異があり同一遺伝子や蛋白の変性という共通経路以外に病態を修飾する因子の関与が推測される。SBMA では高度な前角細胞脱落を示すが、残存運動ニューロンは萎縮しながらもニッスル小体が比較的明瞭で背景には線維性グリオーシスを認める。IC2 陽性構造物を少数の細胞の核内や胞体内に認める。骨格筋は神経原筋萎縮を示す一方、中心核の増加、肥大して残存するものが目立ち、前角細胞の脱落に比して骨格筋はむしろ神経再支配、あるいは代償性肥大により保たれる傾向を示す。ALS では短期間に高度な細胞脱落に至り、肥胖性アストロサイト、macrophage の集簇像を認め、残存する細胞には TDP-43 陽性封入体を認める。骨格筋の神経原性筋萎縮は前角細胞の脱落にほぼ並行する萎縮を示す。

D. 考察

SBMA と ALS では下位運動ニューロンの脱落の速度、蓄積蛋白の違いという病態の違いに加えて、神経支配をうける骨格筋の反応性、あるいは軸索末端の反応に大きな差異がある可能性が示唆される。治療戦略として運動ニューロンの救済に加えて、効果器である骨格筋の保護や刺激なども病態を変えうる可能性がある。

E. 結論

下位運動ニューロンの中枢での軸索脱落と末梢効果器の骨格筋の変性には SBMA と ALS では相違があり、修飾因子の解明が病態や治療の端緒となる可能性があり、iPS 細胞での検証が必要である。

F. 健康危険情報

特になし

G. 研究発表

１．論文発表

1. **Tatsumi S, Mimuro M, Iwasaki Y, Takahashi R, Kakita A, Takahashi H, Yoshida M.** Argyrophilic grains are reliable disease-specific features of corticobasal degeneration. *J Neuropathol Exp Neurol* 73(1):30-38, 2014
2. **Riku Y, Watanabe H, Yoshida M, Tatsumi S, Mimuro M, Iwasaki Y, Katsuno M, Iguchi Y, Masuda M, Senda J, Ishigaki S, Udagawa T, Sobue G.** Lower motor neuron involvement in TAR DNA-binding protein of 43 kDa-related frontotemporal lobar degeneration and amyotrophic lateral sclerosis. *JAMA Neurol.* 71(2):172-9, 2014
3. **Kuru S, Yoshsida M, Tatsumi S, Mimuro M.** Immunohistochemical localization of spatacsin in α-synucleinopathies. *Neuropathology* 34:135-139, 2014
4. **Riku Y, Atsuta N, Yoshida M, Tatsumi S, Iwasaki Y, Mimuro M, Watanabe H, Ito M, Senda J, Nakamura R, Koike H, Sobue G.** Differential motor neuron involvement in progressive muscular atrophy: a comparative study with amyotrophic lateral sclerosis. *BMJ Open* 4: e005213, 2014
5. **Yoshida M.** Astrocytic inclusions in progressive supranuclear palsy and corticobasal degeneration. *Neuropathology.* 34(6):555-70. 2014
6. **Tatsumi S, Uchihara T, Aiba I, Iwasaki Y, Mimuro M, Takahashi R, Yoshida M.** Ultrastructural differences in pretangles between Alzheimer disease and corticobasal degeneration revealed by comparative light and electron microscopy. *Acta Neuropathol Com* **2**:161, 2014
7. **Riku Y, Ando T, Goto Y, Mano K, Iwasaki Y, Sobue G, Yoshida M.** Early pathologic changes in hereditary diffuse leukoencephalopathy with spheroids. *J Neuropathol Exp Neurol.* 73(12):1183-90. 2014

２．学会発表

1. **Yoshida M**. Progressive supranuclear palsy and corticobasal degeneration. XVIII International congress of neuropathology Rio de Janeiro Brazil, 2014 年 9 月

H. 知的財産の出願・登録状況

１．特許取得・出願

なし

２．実用新案登録

なし

３．その他

なし

様式第１９

学　会　等　発　表　実　績

委託業務題目「疾患特異的iPS細胞を用いた球脊髄性筋萎縮症の病態解析と新規治療法の開発」
機関名 学校法人愛知医科大学、国立大学法人名古屋大学、学校法人慶應義塾

１．学会等における口頭・ポスター発表

発表した成果（発表題目、口頭・ポスター発表の別）	発表者氏名	発表した場所（学会等名）	発表した時期	国内・外の別
Incompletely reprogrammed human iPSCs form glioma-like tumors through genomic instability during differentiation. （口頭）	**Okada Y**	Kyoto University /Keio Universiy /MD Anderson Cancer Center (MDACC) Joint Conference, iPS and Stem Cells in Cancer Research, Kyoto, Japan	2014年4月	国際
Application of pluripotent stem cells to the research on neurological disorders. (口頭)	**Okada Y**	2014 KALAS international symposium, Yeosu, Korea	2014年8月	国際
Dysmyelination and Enhanced ER Stress Response in Pelizaeus-Merzbacher Diease Patients iPSCs-Derived Oligodendrocytes with PLP1 Gene Missense Mutations. （口頭）	Numasawa Y, **Okada Y**, Shibata S, Kawabata S, Nakamura M, Kishi N, Akamatsu W, Oyama M, Osaka H, Inoue K, Takahashi K, Yamanaka S, Kosaki K, Takahashi T, Okano H	Neuroscience 2014, Washington DC, USA	2014年11月	国際
白質ジストロフィーの病態研究と問題点 （口頭）	沼澤佑子、**岡田洋平**、芝田晋介、川端走野、中村雅也、岸憲幸、赤松和土、大山学、小坂仁、井上健、高橋和利、山中伸弥、小崎健次郎、高橋孝雄、岡野栄之	第56回小児神経学会学術集会、浜松	2014年5月	国内
多能性幹細胞（ES細胞・iPS細胞）を用いた神経再生とその問題点 (口頭)	**岡田洋平**	第3回長久手脊椎脊髄セミナー、長久手	2014年7月	国内

iPS細胞を用いた神経疾患研究 （口頭）	**岡田洋平**	新潟パーキンソン病治療研究会、新潟	2014年11月	国内
iPS細胞を用いた神経疾患研究 （口頭）	**岡田洋平**	日本神経学会中国四国地方会、広島	2014年12月	国内
Pluripotent Stem Cells and Neurological disorders. （口頭）	**Okada Y**	Distinctive educational program 2014 Neuroscience Course, Nagoya	2014年12月	国内
疾患特異的iPS細胞を用いた神経疾患研究 （口頭）	**岡田洋平**	第１７回ヒューマンサイエス総合研究ワークショップ「再生医療をビジネスへ―細胞治療と周辺事業の新展開―」、東京	2015年1月	国内
疾患特異的iPS細胞を用いた球脊髄性筋萎縮症（SBMA）の病態解析 （ポスター）	小野寺一成、下門大祐、鳥居由紀子、石原康晴、勝野雅央、道勇学、祖父江元、岡野栄之、**岡田洋平**	第14回日本再生医療学会総会、横浜	2015年3月	国内
疾患特異的iPS細胞を用いたニューロマスキュラーハゾロジーの解析 （ポスター）	下門大祐、小野寺一成、石原康晴、勝野雅央、祖父江元、岡野栄之、**岡田洋平**	第14回日本再生医療学会総会、横浜	2015年3月	国内
脳卒中急性期における自律神経機能-電子瞳孔計による対光反応とCVRRの関連 （ポスター）	比嘉智子、中島康自、桑原千秋、安藤宏明、湯淺知子、安本明弘、田口宗太郎、田邉奈千、角田由華、藤掛彰史、徳井啓介、丹羽淳一、泉　雅之、中尾直樹、**道勇　学**	第55回日本神経学会学術大会、福岡	2014年5月	国内
脳卒中に対する急性期リハビリテーションの効果 （口頭）	家田一文、林　博教、橋詰玉枝子、木村伸也、河尻博幸、柳瀬敦志、泉　雅之、丹羽淳一、**道勇　学**	第51回日本リハビリテーション医学学会学術集会、名古屋	2014年6月	国内

Androgen-dependent deficits in muscle-derived BDNF correlate with motor dysfunction in two mouse models of spinal bulbar muscular atrophy. (ポスター)	Halievski K, Xu Y, Henley CL, **Katsuno M**, Adachi H, **Sobue G**, Breedlove S, Jordan CL.	Neuroscience 2014, Washington DC, USA.	2014年11月	国際
SBMA motor dysfunction may be due to failed neuromuscular transmission. (ポスター)	Xu Y, Atchison W, Adachi H, **Katsuno M**, **Sobue G**, Breedlove S, Jordan CL.	Neuroscience 2014, Washington DC, USA	2014年11月	国際
Muscle-specific Control Of Hsp70 In Polyglutamine Induced Motor Neuron Disease. (ポスター)	Kondo N, **Katsuno M**, Adachi H, Sahashi K, Miyazaki Y, Iida M, Tohnai G, Ishigaki S, Fujioka Y, Tanaka F, **Sobue G**.	25th International symposium on ALS/MND, Brussel, Belgium	2014年12月	国際
アンチセンス核酸を用いた球脊髄性筋萎縮症の病態、治療研究 (口演)	佐橋健太郎、**勝野雅央**、Hung Gene、足立弘明、近藤直英、飯田円、中辻秀朗、宮崎雄、藤内玄規、C. Frank Bennett、**祖父江元**	第55回日本神経学会学術大会、福岡	2014年5月	国内
TGF-βシグナル阻害による運動ニューロン変性の病態 (ポスター)	勝又 竜、**勝野雅央**、足立弘明、近藤直英、飯田 円、中辻 秀朗、宮崎 雄、藤内玄規、**祖父江 元**	第55回日本神経学会学術大会、福岡	2014年5月	国内
DNAメチル化阻害剤が球脊髄性筋萎縮症の病態に与える影響の解析 (ポスター)	近藤直英、**勝野雅央**、足立弘明、佐橋健太郎、宮崎雄, 飯田円、藤内玄規、石垣診祐、藤岡祐介、田中章景、**祖父江元**	第55回日本神経学会学術大会、福岡	2014年5月	国内

運動ニューロン疾患における耐糖能異常の解析 （ポスター）	荒木周、 中辻秀朗、 **勝野雅央**、 鈴木啓介、 坂野晴彦、 須賀徳明、 橋詰淳、 土方靖浩、 **祖父江元**	第55回日本神経学会学術大会、福岡	2014年5月	国内
HITS-CLIP reveals multi-layered RNA regulation by translational regulator Msi1 in brain. （ポスター）	**Yano M**, Koya I, Ohtsyka T, Banno S, Yano Y, Robert B. Darnell RB, Okano H	Cold Spring Harbor Meeting, New York, USA	2014年9月	国際
Transcriptome-wide mapping of Msi1-RNA interaction uncovers multi-layered RNA regulation by Msi1 in brain. （口頭）	**矢野真人**、 古家育子、 大塚貴文、 坂野聡重、 矢野佳芳、 ダーネル・ロバート、 岡野栄之	第16回日本RNA学会、名古屋	2014年7月	国内
Musashi, a post-transcriptional regulator of stem cells functions. （口頭）	岡野栄之、 **矢野真人**	第37回 日本神経科学学会、横浜	2014年9月	国内
Roles of neuronal RNA binding protein Elavl2 in the brain. （ポスター）	大塚貴文、 **矢野真人**、 坂野聡重、 芝田晋介、 岡野栄之	第57回日本神経化学会、 奈良	2014年9月	国内
Transcriptome wide mapping of Msi1-RNA interaction in neural stem cell. （口頭）	**矢野真人**、 ダーネル・ロバート、 岡野栄之	第37回 日本分子生物学会、横浜	2014年12月	国内
疾患由来iPS細胞を用いた家族性筋萎縮性側索硬化症の病態解析 （ポスター）	一柳直希、 藤崎央子、 **矢野真人**、 **岡田洋平**、 割田仁、 青木正志、 赤松和土、 岡野栄之	第14回 日本再生医療学会、横浜	2015年3月	国内
Progressive supranuclear palsy and corticobasal degeneration. （口頭）	**Yoshida M**	XVIII International congress of neuropathology	2014年9月	国際

２．学会誌・雑誌等における論文掲載

掲載した論文（発表題目）	発表者氏名	発表した場所 （学会誌・雑誌等名）	発表した時期	国内・外の別
Involvement of ER Stress in Dysmyelination of Pelizaeus-Merzbacher Disease with PLP1 Missense Mutations Shown by iPSC-Derived Oligodendrocytes.	Numasawa-Kuroiwa Y, **Okada Y**, Shibata S, Kishi N, Akamatsu W, Shoji M, Nakanishi A, Oyama M, Osaka H, Inoue K, Takahashi K, Yamanaka S, Kosaki K, Takahashi T, Okano H.	Stem Cell Reports. 2(5) 648-661.	2014年4月	国際
Pathological roles of the VEGF/SphK pathway in Niemann-Pick Type C neurons.	Lee H, Lee JK , Park. MH, Hong YR, Marti H , Kim H, **Okada Y**, Otsu M, Seo E, Park J, Bae JH, Okino N, He X, Schuchman E, Bae J, Jin HK	Nat. Commun. 5:5514.	2014年11月	国際
Utility of Scalp Hair Follicles as a Novel Source of Biomarker Genes for Psychiatric Illnesses.	Maekawa M, Yamada K, Toyoshima M, Ohnishi T, Iwayama Y, Shimamoto C, Toyota T, Nozaki Y, Balan S, Matsuzaki H, Iwata Y, Suzuki K, Miyashita M, Kikuchi M, Kato M, **Okada Y**, Akamatsu W, Norio Mori N, Owada Y, Itokawa M, Okano H, Yoshikawa T	Biological Psychiatry, in press.	2014年9月	国際

Long-term safety issues of iPSC-based cell therapy in a spinal cord injury model: oncogenic transformation with epithelial-mesenchymal transition.	Nori S, **Okada Y**, Nishimura S, Sasaki T, Itakura G, Kobayashi Y, Renault-Mihara F, Shimizu A, Koya I, Yoshida R, Kudo J, Koike M, Uchiyama Y, Ikeda E, Toyama Y, Nakamura M, Okano H	Stem Cell Reports, 4(3) 360-373	2015年3月	国際
iPS細胞創薬への期待と課題	**岡田洋平**、小野寺一成	Frontiers in Parkinson Disease 7(4) 204-208	2014年11月	国内
小児神経疾患克服へ向けた疾患iPS細胞研究の進歩と課題	沼澤佑子、**岡野洋平**、岡野栄之	実験医学増刊号 Vol.33, No.2, 2015	2015年1月	国内
Confirmatory double-blind, parallel-group, placebo-controlled study of efficacy and safety of edaravone(MCI-186) in amyotrophic lateral sclerosis patients.	Abe K, Itoyama Y, Sobue G, Tsuji S, Aoki M, **Doyu M**, Hamada C, Kondo K, Yoneoka T, Akimoto M Yoshino H	Amyotrophic Lateral Sclerosis and Frontotemporal Degeneration, 15(7-8):610-7	2014年12月	国際
Pioglitazone suppresses neuronal and muscular degeneration caused by polyglutamine-expanded androgen receptors.	Iida M, **Katsuno M**, Nakatsuji H, Adachi H, Kondo N, Miyazaki Y, Tohnai G, Ikenaka K, Watanabe H, Yamamoto M, Kishida K, **Sobue G**.	Hum Mol Genet. 24(2) 314-329 2015.	2015年1月	国際

Brugada syndrome in spinal and bulbar muscular atrophy.	Araki A, **Katsuno M**, Suzuki K, Banno H, Suga N, Hashizume A, Mano T, Hijikata Y, Nakatsuji H, Watanabe H, Yamamoto M, Makiyama T, Ohno S, Fukuyama M, Morimoto S, Horie M, **Sobue G**	Neurology. 82(20) 1813-1821, 2014.	2014年5月	国際
Anti-androgen flutamide protects male mice from androgen-dependent toxicity in three models of spinal bulbar muscular atrophy.	Renier KJ, Troxell-Smith SM, Johansen JA, **Katsuno M**, Adachi H, **Sobue G**, Chua JP, Sun Kim H, Lieberman AP, Breedlove SM,	Endocrinology. 155(7) 2624-2634, 2014.	2014年7月	国際
Paeoniflorin eliminates a mutant AR via NF-YA-dependent proteolysis in spinal and bulbar muscular atrophy.	Tohnai G, Adachi H, **Katsuno M**, Doi H, Matsumoto S, Kondo N, Miyazaki Y, Iida M, Nakatsuji H, Qiang Q, Ding Y, Watanabe H, Yamamoto M, Ohtsuka K, **Sobue G**	Hum Mol Genet. 23(13) 3552-3565, 2014.	2014年7月	国際
Potential therapeutic targets in polyglutamine-mediated diseases.	**Katsuno M**, Watanabe H, Yamamoto M, **Sobue G**.	Expert Rev Neurother. 14(10) 1215-1228, 2014.	2014年10月	国際
RNA-binding protein research with transcriptome-wide technologies in neural development.	**Yano M**, Ohtsuka T, Okano H	Cell and Tissue Research, 359(1):135-144 2015	2015年1月	国際
Alternative role of HuD splicing variants in neuronal differentiation.	Hayashi S, **Yano M**, Igarashi M, Okano HJ, Okano H	Journal of Neuroscience Research, 93(3):399-409 2015	2015年3月	国際

Immunohistochemical localization of spatacsin in α-synucleinopathies.	Kuru S, **Yoshsida M**, Tatsumi S, Mimuro M	Neuropathology, 34:135-139,	2014年9月	国際
Differential motor neuron involvement in progressive muscular atrophy: a comparative study with amyotrophic lateral sclerosis.	Riku Y, Atsuta N, **Yoshida M**, Tatsumi S, Iwasaki Y, Mimuro M, Watanabe H, Ito M, Senda J, Nakamura R, Koike H, **Sobue G**	BMJ Open, 4: e005213	2014年5月	国際
Astrocytic inclusions in progressive supranuclear palsy and corticobasal degeneration.	**Yoshida M**	Neuropathology, 34(6):555-70	2014年12月	国際
Ultrastructural differences in pretangles between Alzheimer disease and corticobasal degeneration revealed by comparative light and electron microscopy.	Tatsumi S, Uchihara T, Aiba I, Iwasaki Y, Mimuro M, Takahashi R, **Yoshida M**	Acta Neuropathol Comm, 2:161	2014年12月	国際
Early pathologic changes in hereditary diffuse leukoencephalopathy with spheroids.	Riku Y, Ando T, Goto Y, Mano K, Iwasaki Y, **Sobue G**, **Yoshida M**	J Neuropathol Exp Neurol, 73(12):1183-90	2014年12月	国際

Stem Cell Reports
Article
ISSCR
OPEN ACCES

Involvement of ER Stress in Dysmyelination of Pelizaeus-Merzbacher Disease with *PLP1* Missense Mutations Shown by iPSC-Derived Oligodendrocytes

Yuko Numasawa-Kuroiwa,[1,2] Yohei Okada,[1,3,*] Shinsuke Shibata,[1] Noriyuki Kishi,[1] Wado Akamatsu,[1] Masanobu Shoji,[4] Atsushi Nakanishi,[4] Manabu Oyama,[5] Hitoshi Osaka,[6] Ken Inoue,[7] Kazutoshi Takahashi,[8] Shinya Yamanaka,[8] Kenjiro Kosaki,[9] Takao Takahashi,[2] and Hideyuki Okano[1,*]

[1]Department of Physiology, School of Medicine, Keio University, 35 Shinanomachi, Shinjuku-ku, Tokyo 160-8582, Japan
[2]Department of Pediatrics, School of Medicine, Keio University, 35 Shinanomachi, Shinjuku-ku, Tokyo 160-8582, Japan
[3]Department of Neurology, School of Medicine, Aichi Medical University, 1-1 Yazako Karimata, Nagakute, Aichi 480-1195, Japan
[4]Advanced Science Research Laboratories, Takeda Pharmaceutical Company Limited, 26-1 Muraoka-Higashi 2-Chome, Fujisawa, Kanagawa 251-8555, Japan
[5]Department of Dermatology, School of Medicine, Keio University, 35 Shinanomachi, Shinjuku-ku, Tokyo 160-8582, Japan
[6]Department of Pediatrics, Jichi Medical School, 3311-1 Yakushiji, Shimotsuke-shi, Tochigi 329-0498, Japan
[7]Department of Mental Retardation and Birth Defect Research, National Institute of Neuroscience, National Center of Neurology and Psychiatry, 4-1-1 Ogawahigashi-machi, Kodaira-shi, Tokyo 187-8551, Japan
[8]Center for Induced Pluripotent Stem Cell Research and Application, Graduate School of Medicine, Institute for Frontier Medical Sciences, Kyoto University, Kyoto 606-8507, Japan
[9]Center for Medical Genetics, School of Medicine, Keio University, 35 Shinanomachi, Shinjuku-ku, Tokyo 160-8582, Japan
*Correspondence: yohei@a6.keio.jp (Y.O.), hidokano@a2.keio.jp (H.O.)
http://dx.doi.org/10.1016/j.stemcr.2014.03.007

SUMMARY

Pelizaeus-Merzbacher disease (PMD) is a form of X-linked leukodystrophy caused by mutations in the *proteolipid protein 1* (*PLP1*) gene. Although PLP1 proteins with missense mutations have been shown to accumulate in the rough endoplasmic reticulum (ER) in disease model animals and cell lines transfected with mutant *PLP1* genes, the exact pathogenetic mechanism of PMD has not previously been clarified. In this study, we established induced pluripotent stem cells (iPSCs) from two PMD patients carrying missense mutation and differentiated them into oligodendrocytes in vitro. In the PMD iPSC-derived oligodendrocytes, mislocalization of mutant PLP1 proteins to the ER and an association between increased susceptibility to ER stress and increased numbers of apoptotic oligodendrocytes were observed. Moreover, electron microscopic analysis demonstrated drastically reduced myelin formation accompanied by abnormal ER morphology. Thus, this study demonstrates the involvement of ER stress in pathogenic dysmyelination in the oligodendrocytes of PMD patients with the *PLP1* missense mutation.

INTRODUCTION

Analysis of differentiated cells from disease-specific, human induced pluripotent stem cells (iPSCs) enables the construction of pathological models using the patients' own cells. Such analyses are particularly useful for the study of neurodegenerative disorders because it is difficult to collect brain-tissue samples from these patients.

Pelizaeus-Merzbacher disease (PMD) is a dysmyelinating disorder of the CNS that is usually observed during childhood. PMD is classified into two subtypes: the classical and connatal forms. In the classical form, patients usually show a delay in psychomotor development within the first year of life but exhibit relatively slow disease progression over the first decade. In contrast, in the connatal form, patients generally show arrested congenital psychomotor development and exhibit a progressive disease course with severe neurological impairment. The degree of dysmyelination has been shown to correlate well with the clinical severity of PMD (Seitelberger, 1995). The *proteolipid protein 1* (*PLP1*) gene has been identified as a causative gene for PMD. PLP1 is a transmembrane protein that is abundantly expressed in compact myelin in oligodendrocytes (OLs) and plays a structural role in the formation and maintenance of myelin sheaths (Gow et al., 1997; Mikoshiba et al., 1991). Three distinct types of *PLP1* mutation have been reported to date: point mutations, duplications, and deletions. Missense mutations in the *PLP1* gene account for 30% of the genetic abnormalities found in PMD patients and are responsible for most of connatal cases. Based on analyses using cell lines transfected with mutant *PLP1* genes (Gow and Lazzarini, 1996) or a mouse model of PMD (the *msd* mouse; Gow et al., 1998), the underlying pathogenesis in most patients with missense mutations is thought to involve the accumulation of misfolded mutant PLP1 proteins in the rough endoplasmic reticulum (ER) (Southwood et al., 2002) and the induction of ER stress, resulting in activation of the unfolded protein response (UPR). Although UPR attenuates general translation to reduce the protein load into ER and increase expression of chaperone proteins to facilitate protein folding, excessive levels of unfolded proteins have been shown to activate apoptotic pathway of UPR to eliminate damaged OLs.

CrossMark

However, despite the precise analyses conducted using conventional cellular and animal PMD models, it has not been possible to examine the actual correlation between the known molecular pathogenesis and cell biological phenotypes, including abnormalities in OL differentiation, myelination, and cell death. In addition, those previous results were obtained through analyses using nonhuman models, non-patient-derived cells, or nonoligodendrocyte models, and it is unknown whether the results obtained in those models are applicable to human patients. Although the establishment of iPSCs from a PMD patient with partial duplication of *PLP1* gene has been reported, those iPSCs were not differentiated into oligodendrocytes for disease modeling (Shimojima et al., 2012). Thus, in the present study, we focused on the pathologic effects of *PLP1* missense mutations and established patient-specific iPSCs from two PMD patients with different mutation sites and different levels of clinical severity.

We differentiated the iPSCs into OL lineage cells and examined the pathogenic changes in the PMD iPSC-derived OLs. We confirmed the accumulation and mislocalization of mutant PLP1 proteins to the ER, a high level of stress susceptibility, and increased apoptosis in PMD iPSC-derived OLs. In addition, through transmission electron microscopic analysis, we verified decreases in the frequency of myelin formation and the thickness of the myelin sheath compared with control cells. More importantly, we also demonstrated that these pathogenic changes observed in iPSC-derived OLs were consistent with the different levels of clinical severity between the two PMD patients. Thus, this report describes the modeling of human PMD with *PLP1* missense mutations using patient-specific, iPSC-derived OLs. These results have demonstrated the usefulness of iPSC-derived OLs for the analysis of the pathogenic processes in human dysmyelinating neurological disorders.

RESULTS

Clinical Features of PMD Patients

We established iPSCs from two patients with point mutations in the transmembrane domain (patient 1: PMD1) and extracellular domain (patient 2: PMD2) of the *PLP1* gene (Figure 1C). PMD1 was a 1-year-old male with the connatal form of PMD. He was diagnosed with PMD at the age of 4 months, when he was found to exhibit poor head control and nystagmus and was unable to follow objects. He showed poor feeding and was fed through a gastrostomy tube from the age of 21 months. Psychomotor development was not observed, even at the age of 5 years. MRI of the patient's brain revealed mild and diffuse atrophy, dilatation of the ventricles, and diffuse high-intensity signals in the white matter of the cerebrum and brainstem in a T2-weighted image (T2WI) (Figure 1A). A direct sequencing analysis of genomic DNA from the patient's leukocytes showed a novel missense mutation, c.757 T > A (p.Ser253Thr), in exon 6 of the *PLP1* gene (Figure 1B). This amino acid change has not been previously reported, but different type of mutation at this same site, Ser253Phe, has been reported in other patients with the connatal form of PMD (Hodes et al., 1998). This change was not identified in more than 200 normal individuals; thus, it was considered to be a causative mutation for PMD.

Patient 2 (PMD2) was a 20-year-old male with the classical form of PMD. He was diagnosed with PMD at the age of 3 months, when he was found to display poor head control and nystagmus. Spastic quadriparesis was evident at 4 years of age, with choreoathetotic movements beginning at the age of 8–10 years. He appeared alert and attentive and was nonverbal but exhibited guttural vocalizations. A missense mutation, c.643 C > T (p.Pro215Ser), was identified in exon 5 of the *PLP1* gene, which has been reported previously (Gencic et al., 1989).

Establishment and Characterization of iPSCs Derived from PMD Patients

Human iPSCs were established via the retroviral transduction of four transcription factors (*SOX2*, *OCT4*, *KLF4*, and *c-MYC*) into dermal fibroblasts (Takahashi et al., 2007). A total of 52 and 34 iPSC clones were established from PMD1 and PMD2 samples, respectively. The established iPSC clones were evaluated based on the typical morphology of colonies similar to human embryonic stem cells (ESCs), as well as the expression of pluripotent markers via immunocytochemistry (NANOG and OCT4; Figure 1D), silencing of retroviral transgenes through quantitative RT-PCR (Figure 1E), and efficient differentiation into neural cells via embryoid body (EB) formation. We finally selected three clones each for PMD1 (1-7, 1-15, and 1-27) and PMD2 (2-6, 2-10, and 2-22) for further analyses. The differentiation potentials of these selected iPSC clones were confirmed through teratoma formation assays (ectoderm: neural rosettes and pigmented epithelium, endoderm: goblet cells, and mesoderm: bones and cartilage; Figure 1F). Moreover, the mutations in the *PLP1* gene (PMD1 [c.757 T > A] and PMD2 [c.643 C > T]) were confirmed in human dermal fibroblasts (HDFs) and all of the selected iPSC clones via pyrosequencing analysis (Figure 1G).

Regarding the control iPSCs, we used age-matched control iPSCs established from 8-month-old (TIG121) and 16-year-old (WD39) healthy individuals, corresponding to the PMD-iPSCs established from 1-year-old and 20-year-old patients, respectively, as well as 201B7, which is a widely used control iPSC clone.

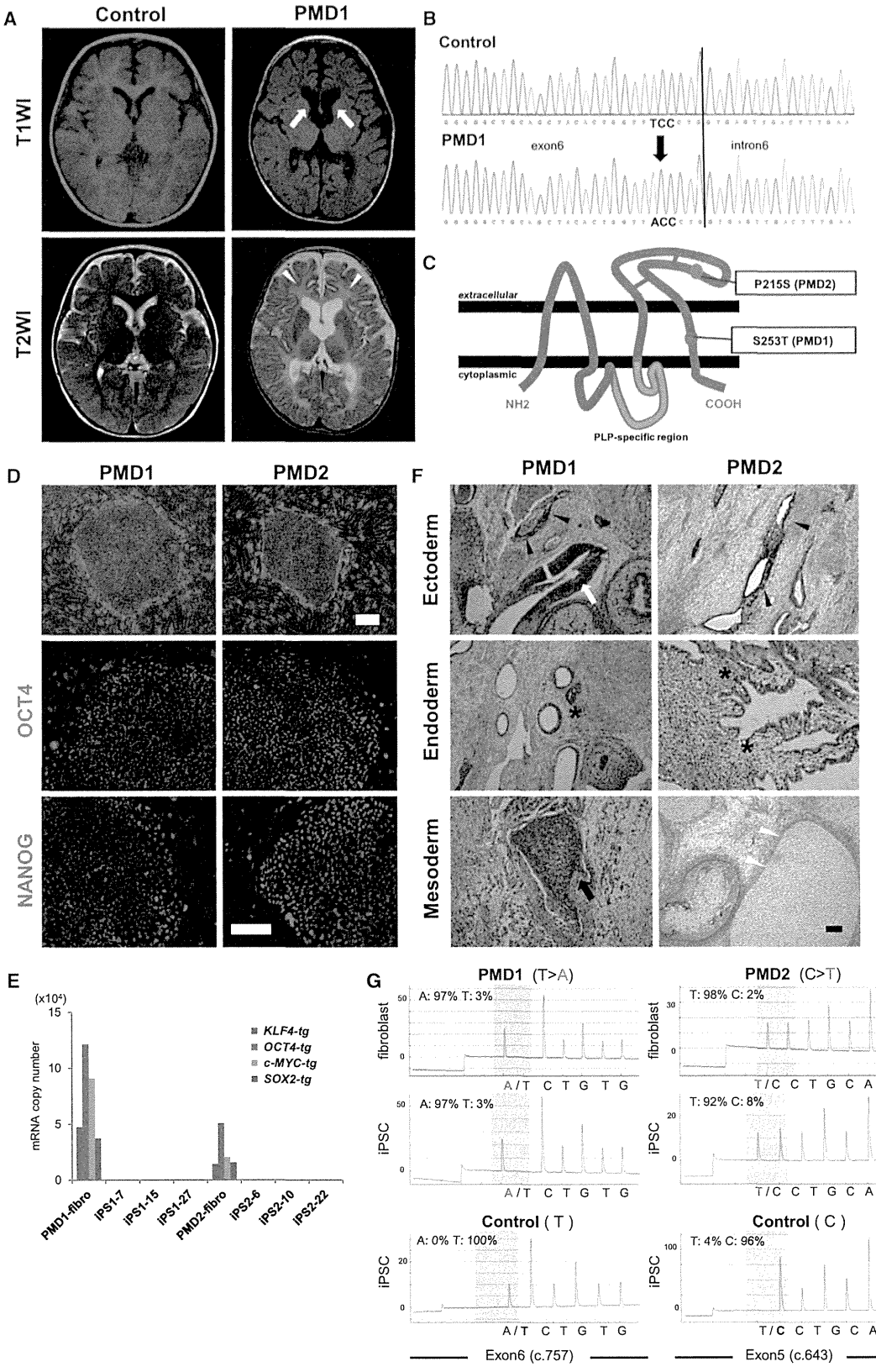

(legend on next page)

Both Control and PMD iPSCs Induce Oligodendrocyte Lineage Cells In Vitro

Based on the previously reported methods for inducing OLs from human ESCs and iPSCs (Hu et al., 2009; Izrael et al., 2007; Kang et al., 2007), we established our own culture protocol to induce OLs by modifying previously established protocols for efficiently differentiating human ESCs and iPSCs into neural stem/progenitor cells (NS/PCs) as neurospheres through EB formation (Nori et al., 2011; Okada et al., 2008). First, dorsomorphin (a bone morphogenetic protein signal inhibitor), SB431542 (a transforming growth factor β [TGF-β] receptor inhibitor), and BIO (a GSK3 inhibitor) were added during the early phase of EB formation to facilitate differentiation into NS/PCs more efficiently. Quantitative RT-PCR analysis of the expression of the NS/PC marker *SOX1* in EBs revealed a significantly higher induction efficiency of NS/PCs in our protocol with DSB (DSB: dorsomorphin, SB431542, and BIO) compared with those in our previously established methods (control, DSB−) or those in the previously reported dual Smad inhibition with DS (Figure 2B). We also added retinoic acid for caudalization and purmorphamine (Sonic hedgehog agonist) for ventralization during EB formation until EB dissociation. Then, the dissociated EBs were cultured in suspension to form neurospheres in proliferation medium supplemented with factors that promote the commitment and proliferation of OL lineage cells (Shimada et al., 2012). For adherent differentiation, neurospheres were cultured in differentiation medium supplemented with factors that promote the commitment of OL lineage cells as indicated in the Experimental Procedures (Figure 2A). From the quantitative RT-PCR analysis in this protocol, the pluripotent marker (*NANOG*) was notably downregulated in the EB stage, and other lineage markers (mesodermal and endodermal markers, such as *BRACHYURY* and *SOX17*) were not detected in any stage. The NS/PC marker (*SOX1*) was upregulated in the EB and neurosphere stages and gradually downregulated after adherent differentiation (differentiation stage; Figure 2C). The expression profiles were similar between the control, PMD1, and PMD2 iPSCs (Figure S1A available online). To reveal the differentiation potentials of neurospheres, we performed immunocytochemistry of differentiated neurospheres for markers of neurons (βIII tubulin), astrocytes (GFAP), and oligodendrocytes (O4; Figures 2E and 2F) and a time course analysis of the expression levels of neuronal and glial markers through quantitative RT-PCR (Figure 2D). The expression profiles were similar between the control and PMD1 and PMD2 cells (Figure S1B). Based on these analyses, we confirmed the differentiation potentials of the iPSCs into three neural lineage cells and the reproducibility of our differentiation protocol. Regarding the differentiation potentials of OL lineage cells, all PMD-iPSCs and control iPSCs were able to induce platelet-derived growth factor receptor α (PDGFRα)$^+$-OL progenitor cells (OPCs), O4$^+$-immature OLs (immature OLs), and myelin basic protein (MBP)$^+$-mature OLs (mature OLs) with typical morphologies (Figure 3B). OPCs were also positive for NG2 (Figure 3A). In contrast, myelin protein zero (MPZ)-positive cells, a major structural protein of peripheral myelin, could not be detected, indicating that these cells were oligodendrocytes, but not schwann cells.

After 55–70 days in vitro (DIV), OPCs were observed in 86.3% of the colonies of control cells and 95.1% and 90.5% of the colonies of PMD1 and PMD2 cells, respectively. At 70–85 DIV, immature OLs were observed in 77.8% of control colonies and 93.8% and 93.8% of the colonies of PMD1 and PMD2 cells, respectively. At 80–95 DIV, mature OLs were observed in 74.9% of the colonies of control cells and 93.8% and 89.2% of the colonies of PMD1 and PMD2 cells, respectively (Figure 3C). No significant

Figure 1. Features of the PMD Patients and Characterization of iPSCs

(A) MRI images of the brains of patient PMD1 (right) and an age-matched control (left). Mild and diffuse atrophy of the brain, dilatation of the ventricles (open arrow), and diffuse high-intensity signals in the white matter (open arrowhead) are shown. T1WI, T1-weighted images; T2WI, T2-weighted images.

(B) Direct sequencing analysis of genomic DNA from PMD1's leukocytes showed a missense mutation c.757 T > A (p.Ser253Thr) in exon 6 of the *PLP1* gene.

(C) Schematic representation of the mutation sites in PMD1 and PMD2.

(D) Representative morphology of iPSC colonies (above) and immunochemical analysis of pluripotent markers, NANOG and OCT4 (below). The scale bars represent 200 μm.

(E) Quantitative RT-PCR analysis of the expression of retroviral transgenes in established PMD iPSC clones. Data are presented as the mRNA copy numbers for each transgene divided by those for *β-actin*.

(F) Representative H&E staining of teratomas derived from established PMD iPSC clones. Teratomas were formed via the injection of undifferentiated iPSCs into the testes of NOD/SCID mice. Open arrow, neural rosettes. Arrowhead, pigmented epitheliums. Asterisks, goblet cells. Arrow, bones. Open arrowhead, cartilage. The scale bars represent 200 μm.

(G) Representative pyrosequencing analysis of the mutations in the *PLP1* gene in fibroblasts and iPSCs. Identical mutations to those observed in the patients' fibroblasts (PMD1, 757 T > A; PMD2, 643 C > T) were confirmed in all the iPSC clones.

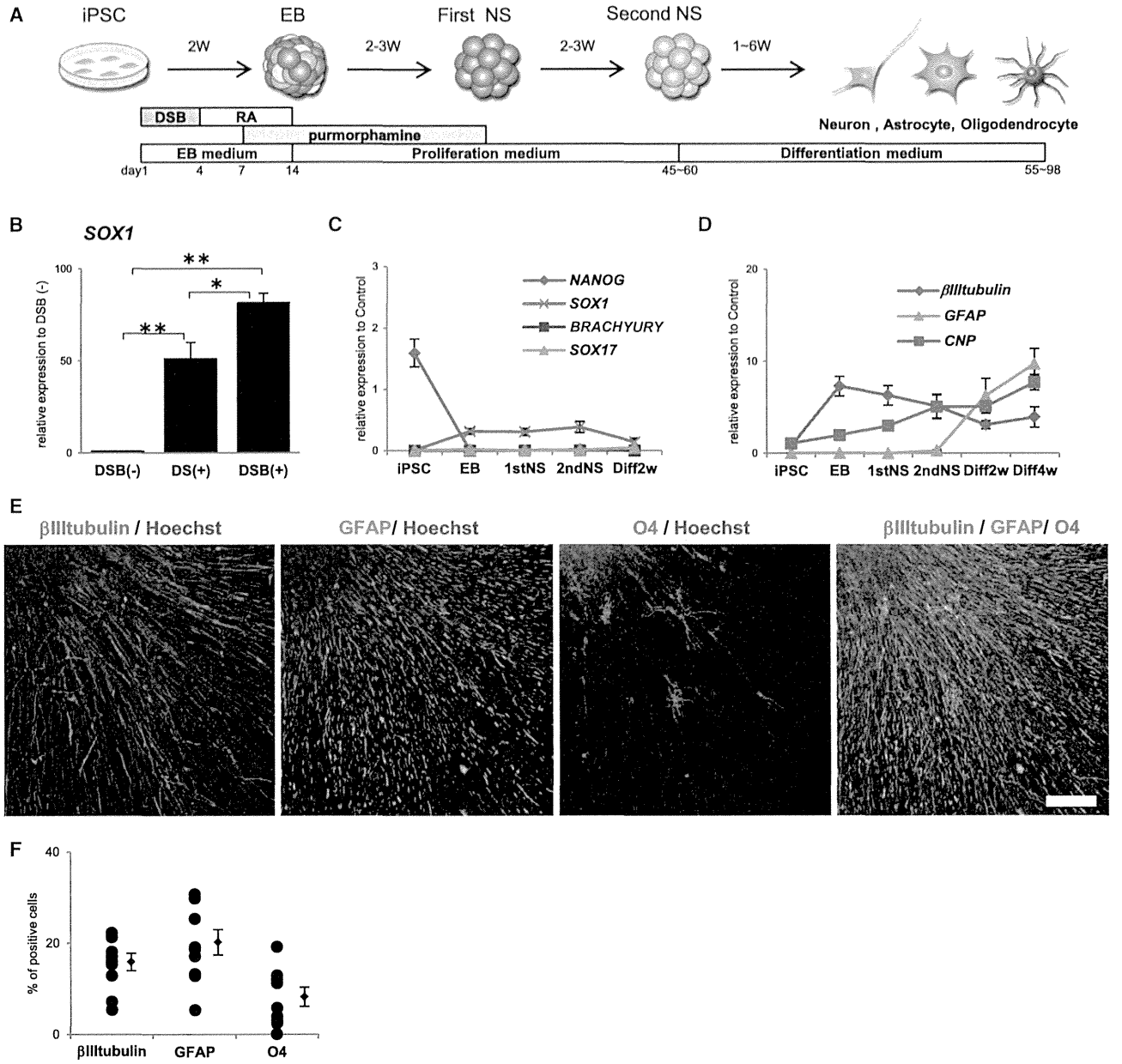

Figure 2. Differentiation Potential of Human iPSCs

(A) Schematic presentation of the protocols for OL differentiation from hiPSCs. DSB, dorsomorphine (D), SB431542 (S), and BIO (B); RA, retinoic acid; NS, neurospheres.

(B) Quantitative RT-PCR analysis of *SOX1* expression in EBs, suggesting a significantly higher induction efficiency of NS/PCs in EBs in our protocol with DSB (DSB: dorsomorphin, SB431542, and BIO) compared with those in our previously established methods (control, DSB−) or those in the previously reported method with dual Smad inhibition (DS) (n = 3, mean ± SEM; independent experiments; *p < 0.05; **p < 0.01; t test).

(C) Quantitative RT-PCR analysis of the expression of cell-type-specific markers at each differentiation stage. *NANOG* (a pluripotent marker) was readily downregulated in the EB stage. Other lineage markers (mesodermal and endodermal markers, such as *BRACHYURY* and *SOX17*) were not detected in any stage. *SOX1* was upregulated in EB and neurosphere stage in control iPSC clones (201B7, WD39, and TIG121; n = 3; mean ± SEM; independent experiments).

(D) Quantitative RT-PCR analysis of differentiated neurospheres for the markers of neurons (*βIII tubulin*), astrocytes (*GFAP*), and oligodendrocytes (*CNP*) in control iPSC clones (201B7, WD39, and TIG121; n = 3; mean ± SEM; independent experiments).

(legend continued on next page)

differences were detected in either control or PMD with regard to OL lineage differentiation efficiency.

To examine the proportion of immature and mature OL lineage cells, we performed immunocytochemistry for OLIG2, PDGFRα, and MBP after 2 or 4 weeks differentiation of control-iPSC-derived second neurospheres containing more than 40 OLIG2-positive cells and counted the number of marker-positive cells (Figures 3D and 3E). After 2 and 4 weeks of differentiation, OLIG2$^+$ and PDGFRα$^+$ OPCs were abundantly observed. After 4 weeks of differentiation, small numbers of MBP$^+$ mature OLs appeared.

Involvement of ER Stress in PMD

Previous in vitro transfection studies in nonglial cells have indicated that various PLP1 mutants accumulate in the ER immediately after translation, in contrast to the distribution of wild-type PLP1 at the plasma membrane (Gow et al., 1994; Gow and Lazzarini, 1996; Thomson et al., 1997). Therefore, we next examined the expression of PLP1 proteins via immunocytochemistry. When stained with anti-PLP1 and MBP antibodies, the membrane protein PLP1 was observed to be dispersed into the processes of OLs and to colocalize with MBP in control iPSC-derived mature OLs. However, in PMD1 and PMD2 iPSC-derived mature OLs, PLP1 protein staining was not observed in the OL processes; instead, PLP1 protein staining localized to the perinuclear cytoplasm (Figure 4A). Thus, we also performed staining for the ER marker KDEL and found that the mislocalized PLP1 proteins colocalized with KDEL (Figures 4A and 4B). All of the control iPSC-derived OLs showed staining for PLP1 proteins in the processes of mature OLs, whereas all of the PMD iPSC-derived mature OLs only exhibited PLP1 protein localization in the ER. These results suggest that mutant PLP1 proteins accumulated in the ER and triggered ER stress in mature OLs derived from PMD-iPSCs.

We next examined the expression of ER stress markers in OLs. O4$^+$ cells were isolated from both the PMD and control iPSC-derived differentiated cells 4 weeks after the attachment of the second neurospheres via magnetic-activated cell sorting (MACS) using an anti-O4 antibody. The purified O4$^+$ cells underwent quantitative RT-PCR to determine the expression of ER stress markers (*BIP*, *CHOP*, and spliced *XBP1*). No significant differences were detected between the control and PMD iPSC-derived OLs regarding the expression of ER stress markers under default conditions (Figure 4C). Therefore, we next examined the susceptibility of the iPSC-derived OLs to the extrinsic ER stress induced by treatment with a low concentration of tunicamycin 50 nM for 6 hr (known as an ER-stress inducer). The results showed that the expression of all ER-stress markers was significantly increased in tunicamycin-treated O4$^+$ cells relative to untreated O4$^+$ cells in PMD1 (Figure 4D). This result suggested that a higher susceptibility to ER stress was observed in PMD1 iPSC-derived OLs than in those derived from control and PMD2 iPSCs.

We next treated the iPSC-derived OLs with a higher concentration of tunicamycin 100 nM for 6 hr and examined the expression levels of ER stress markers. PMD2 iPSC-derived OLs showed significantly higher expression levels of spliced *XBP1*, the most sensitive ER stress marker, than control iPSC-derived OLs (Figure 4E). No significant differences were detected in the expression levels of *BIP* and *CHOP* between control and PMD2. Taken together, these results suggest that ER stress is involved in the pathogenesis of the PMD patients with PLP1 missense mutations, and a higher susceptibility to ER stress was observed in PMD1 iPSC-derived OLs than in those derived from PMD2, which is consistent with the more severe phenotypes of the PMD1 patient compared with the PMD2 patient.

Increased Apoptosis Is Observed in PMD iPSC-Derived Oligodendrocytes

In addition to their susceptibility to ER stress, the PMD iPSC-derived OLs showed significant morphological differences, as revealed by O4 staining, such as scattered O4 staining in their processes compared with control iPSC-derived OLs, which exhibited uniform O4 staining in their processes (Figure 5A). Thus, to investigate the apoptotic processes of PMD iPSC-derived OL lineage cells, we examined the expression of cleaved caspase-3 (apoptotic marker) in O4$^+$-immature OLs and MBP$^+$-mature OLs via immunostaining. Some of the PMD iPSC-derived OLs that showed scattered O4 staining in their processes were positive for cleaved caspase-3 (Figure 5B). The numbers of cleaved caspase-3$^+$ cells in both PMD1 and PMD2 iPSC-derived immature OLs and mature OLs were significantly increased compared with those derived from control iPSCs (Figure 5C). We next performed immunocytochemistry for KI67 and OLIG2. We found that the proportion of OLIG2$^+$ cells and KI67$^+$ cells among OLIG2$^+$ cells were unchanged between PMD and control samples, suggesting that the compensatory proliferation of OPCs for increased apoptosis in PMD iPSC-derived OLs is unlikely (Figures S2A and S2B). Therefore, although

(E) Representative low-magnification images of the immunocytochemistry of three neural lineage cells (neurons: βIII tubulin; astrocytes: GFAP; oligodendrocytes: O4). The scale bar represents 100 μm.
(F) Quantitative analysis of the percentages of three neural lineage cells in control-iPSCs (201B7, WD39, and TIG121)-derived neurospheres (n = 9; mean ± SEM; independent experiments).

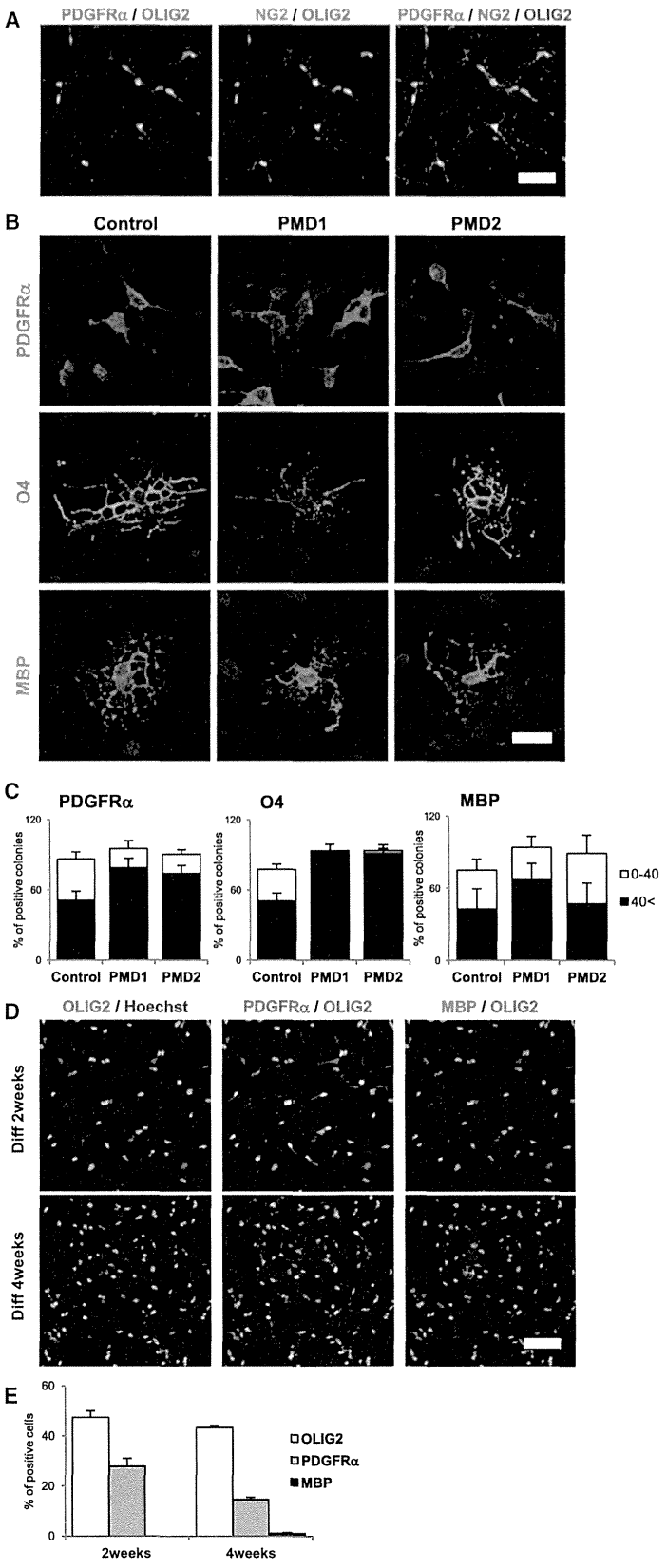

Figure 3. Differentiation Potential of Human iPSCs into Oligodendrocytes

(A) Representative image of immunocytochemistry for OPC markers (PDGFRα and NG2). OPCs were positive for both PDGFRα and NG2. The scale bar represents 50 μm.

(B) Representative image of immunocytochemistry of differentiated neurospheres using markers for OL lineage cells. Both control and PMD iPSCs differentiated into PDGFRα$^+$-OL progenitor cells (OPCs), O4$^+$-immature OLs (immature OLs), and MBP$^+$-mature OLs (mature OLs). The scale bar represents 20 μm.

(C) Quantitative analysis of the differentiation efficiency into OL lineage cells. The numbers of neurosphere colonies containing more than 40 marker-positive cells ($\geq$40 cells; oligodendrocyte [++]), those containing less than 40 marker-positive cells (1–39 cells oligodendrocyte [+]), and those without marker-positive cells (oligodendrocyte [−]) were counted and are presented as the percentage of total neurosphere colonies. Oligodendrocyte (++) neurosphere colonies and oligodendrocyte (+) neurosphere colonies are indicated by black and white bars, respectively (PDGFRα, n = 6; O4, n = 6; MBP, n = 4; mean ± SEM; independent experiments). No significant difference was detected among control (201B7, WD39, and TIG121) and PMD iPSCs (PMD1-7, PMD1-15, and PMD1-27 and PMD2-6, PMD2-10, and PMD2-22)-derived OL lineage cells ($p > 0.05$; Mann-Whitney's U test).

(D) Representative image of immunocytochemistry for OLIG2, PDGFRα, and MBP after 2 or 4 weeks differentiation of control-iPSC-derived second neurospheres containing more than 40 OLIG2-positive cells. The scale bar represents 50 μm.

(E) Quantitative data of the percentages of PDGFRα$^+$ cells/OLIG2$^+$ cells and MBP$^+$ cells/OLIG2$^+$ cells (after 2 or 4 weeks of differentiation) in control-iPSC (201B7, WD39, and TIG121)-derived neurospheres containing more than 40 OLIG2-positive cells. (n = 3; mean ± SEM; independent experiments). After 2 and 4 weeks of differentiation, OLIG2$^+$ and PDGFRα$^+$ OPCs were abundantly observed. After 4 weeks of differentiation, small numbers of MBP$^+$ mature OLs appeared.